Improved Modeling of Thioamide FRET Quenching

by Including Conformational Restriction and

Coulomb Coupling

Jimin Yoon[†], John J. Ferrie^{‡*}, E. James Petersson*

Department of Chemistry, University of Pennsylvania, Philadelphia, Pennsylvania, 19104,

United States

Keywords: Förster resonance energy transfer, thioamide, fluorescence quenching, molecular modeling, Rosetta

ABSTRACT

Thioamide containing amino acids have been shown to quench a wide range of fluorophores through distinct mechanisms. Here, we quantitatively analyze the mechanism through which the thioamide functional group quenches the fluorescence of *p*-cyanophenylalanine (Cnf), tyrosine (Tyr) and tryptophan (Trp). By comparing PyRosetta simulations to published experiments performed on polyproline ruler peptides, we corroborate previous findings that both Cnf and Tyr quenching occurs via Förster resonance energy transfer (FRET), while Trp quenching occurs through an alternate mechanism such as Dexter transfer. Additionally, optimization of the peptide

sampling scheme and comparison of thioamides attached to the peptide backbone and sidechain revealed that the significant conformational restriction associated with the thioamide moiety results in a high sensitivity of the apparent FRET efficiency to underlying conformational differences. Moreover, by computing FRET efficiencies from structural models using a variety of approaches, we find that quantitative accuracy in the role of Coulomb coupling is required to explain contributions to the observed quenching efficiency from individual structures on a detailed level. Lastly, we demonstrate that these additional considerations improve our ability to predict thioamide quenching efficiencies observed during binding of thioamide labeled peptides to fluorophore labeled variants of calmodulin.

INTRODUCTION

Fluorescence spectroscopy has been used as an effective tool in biophysics for a variety of purposes.¹ In particular, energy transfer from donor to acceptor probes has been used to study macromolecular structure-function relationships, as the extent of transfer through mechanisms such as Förster resonance energy transfer (FRET) can be used to calculate the distance between the probes under varying experimental conditions.²⁻⁴ These techniques have helped to elucidate the dynamics of biological macromolecules⁵⁻⁶ and their binding interactions,⁷⁻⁸ as well as the molecular mechanisms of protein folding and misfolding.⁹⁻¹⁰

Common mathematical formulations of the FRET phenomenon assume that the two dyes, a "donor" and "acceptor", interact as spatially separated dipoles whose electronic coupling gives rise to non-radiative decay of the initially excited donor dye.¹ Although FRET is most sensitive to the inter-probe distance, other factors including the local dielectric, the donor fluorophore quantum yield and the orientational sampling of each probe can complicate the assignment of discrete distance values from observed FRET efficiencies.¹¹¹-¹³ Despite the fact that many of these values

can be determined empirically, precisely measuring the dipole orientation factor (κ^2) has been a long-standing problem.¹⁴ Although chromophore orientations can be partially deduced from fluorescence polarization anisotropy,¹⁵⁻¹⁶ and κ^2 values have been estimated for a limited number of protein systems,¹⁷⁻¹⁸ explicit determination remains difficult. Theoretically, κ^2 can be approximated as equal to 2/3 when the isotropic condition (chromophore orientations are distributed uniformly) and the dynamic averaging condition (the timescale of rotational diffusion of chromophores is much shorter than the lifetime of donor fluorophore) are both met.^{1,14,18} This model of FRET, termed the Point Dipole Approximation (PDA), accurately describes widely studied systems which utilize flexible probes separated by relatively large distances. However, the assumption can be problematic for small, conformationally restricted fluorophores and those that have relatively short lifetimes.¹⁹

One major limitation of the PDA is that it does not accurately account for the Coulomb coupling experienced by one chromophore due to the transition density of another, which is significant at short distances.¹² Recently, work by Sobakinskaya and coworkers demonstrated that indeed using the transition charge from electrostatic potential (TrESP) method, which allows for calculation of the Coulomb coupling by accounting for excitonic couplings, improves the prediction of FRET efficiencies, in particular at shorter distances (< 40 Å).¹²

Beyond probe-specific considerations, accurate protein modeling is crucial to ensure FRET data are correctly interpreted.^{13, 20} Systems once thought to be rigid can have structural properties that need to be thoughtfully considered in order to generate accurate and representative models. For instance, re-evaluation of FRET studies performed using "molecular rulers", such as the polyproline peptide model system, has demonstrated unsuspected complexity in the sampling of *cis* amide bonds in prolines and other conformational biases.^{12, 21-23}

In this work, we focus on understanding the degree to which anisotropic sampling and excitonic coupling contribute to the FRET efficiencies observed between small fluorophores and a thioamide quencher. A thioamide is an amide oxygen-to-sulfur substitution in the backbone or sidechain of an amino acid. Importantly, the thioamide has been shown to quench the fluorescence of small, UV fluorophores including p-cyanophenylalanine (Cnf), tyrosine (Tyr) and tryptophan (Trp).^{4,24} ²⁵ Previous empirical studies of these fluorophore-quencher systems suggested that both Cnf and Tyr interact with the thioamide through FRET, while Trp interacts through some alternative mechanism (either Dexter transfer at short range or long-range electron transfer involving transient radicals, which we have shown to be operational for red-shifted fluorophores²⁶). Modeling protein and peptide conformation through short molecular dynamics (MD) trajectories provided moderate agreement with experiment, but some deviations from predicted FRET values could not be rationalized. We hypothesized that a rigorous understanding of probe dynamics and the role of Coulomb coupling is necessary to computationally simulate thioamide-containing systems.^{4, 25} Using Monte Carlo based simulations in PyRosetta, we successfully demonstrate that for peptide/protein systems with known low-energy structure(s) optimizing the conformational sampling and accounting for Coulomb coupling yield a major improvement in the accuracy of computationally predicted FRET efficiencies in Cnf and Tyr probe studies.²⁷ Additionally, we observe that accounting for these additional complexities is unable to explain the behavior observed for Trp-thioamide interactions, which are primarily non-FRET interactions. Lastly, we demonstrate that detailed accounting of Coulomb coupling via the TrESP method improves our ability to predict observed FRET efficiencies in calmodulin/peptide (CaM/pOCNC) binding studies.⁴ Overall, these findings support two important conclusions. First, relatively short-range FRET interactions between small chromophores are not effectively modeled using classical

approximations. Second, including realistic conformational modeling with explicit treatment of Coulomb coupling can provide much more accurate models of FRET in these systems.

METHODS

All simulations were performed in PyRosetta and detailed descriptions of computational code and analyses are provided in the Supporting Information (SI).²⁷ Here, we outline the design considerations in our simulations to guide the subsequent reporting of results and discussion.

Residue Specific Parameters Files. Rosetta residue parameter files were constructed for generating thionated versions of all 20 canonical amino acids based on optimized geometries and charges from N-acetyl-L-alanine methylthioamide. Gaussian09 geometry optimization calculations were performed at the Hartree-Fock (HF) level using the 6-31g (d) basis set, as previously described.²⁸⁻²⁹ The parent amino acid parameter file was adjusted by setting the oxygen atom to a virtual atom (which is not considered when energies are computed) and introducing the new sulfur atom at C-S bond length determined from the N-acetylalanine methylthioamide Gaussian09 output. All backbone atom charges were adjusted to those computed using the CHELPG method in Gaussian 09.30 To specifically adjust the charge of the backbone nitrogen for the residue subsequent (i+1) to the thioamide, a patch file containing the new charge values was applied. All other aspects of the thioamide-containing amino acid parameter files remain unchanged from those of the parent amino acid libraries, including the backbone-dependent rotamer libraries. Additionally, the same geometric and chemical properties were used to generate the sidechain thioamide, thioacetyl lysine (Lys(Ac^S)) patch file from the acetyl lysine patch file in Rosetta. Lastly, the p-cyano substitution of phenylalanine for simulating (Cnf) was already available as a patch file in Rosetta.

PolyProline Simulations. All polyproline simulations used the polyproline type-II helix (PPII) as a starting structure, where the number of prolines varied from 2 to 10 for Leu^S (where the superscript S denotes the thioamide), and 2 to 6 for Lys(Ac^S).^{24-25,31} To match prior experiments, the backbone thioamide containing polyproline structures contained Cnf/Tyr/Trp at the N-terminus and the thioleucine (Leu^S) at the C-terminus, while sidechain thioamide containing polyproline structures contained Lys(Ac^S) at the N-terminus and Cnf/Trp at the C-terminus. ^{24-25,31}

Previously, Backrub simulations have been shown to produce structure ensembles that mimic solution-phase dynamics by sampling local motions via rotations around axes defined by two backbone atoms. $^{32-33}$ Using a modified Backrub-based sampling method implemented in PyRosetta, 1000 unique backbone and sidechain conformations were generated via torsional sampling. This simulation scheme comprises the base simulation referred to in text as *PPII*. To this, we applied probabilistic sampling to randomize input rotamers of sidechains (+ *Chi Sampling*), to sample cisPro conformations (+ *Internal cisPro*), to specifically adjust sampling for terminal prolines (+ *Terminal cisPro*), and favor sampling of geometries consistent with backbone-sidechain CH- π interactions (+ *CH-\pi Interaction*). These methods were used to generate 100 unique structures for each starting backbone conformation, which were then subjected to gradient-based minimization. The minimization produced an ensemble consisting of 100,000 final structures. Additional details are provided in the SI.

CaM/pOCNC Simulations. Simulations of the CaM/pOCNC system were performed in PyRosetta using the canonical Backrub simulation format under the REF2015 scorefunction. Previously reported solution-phase NMR structures (PDB 1SY9) were relaxed and used as input structures, where mutations were introduced using the MutateResidue mover. The sampling improvements made for the polyproline system (+ Internal cisPro, + Terminal cisPro, + CH- π

Interaction) were not applied to the CaM/pOCNC complex for the lack of experimental data showing the isomerization probability specifically of proline residues. The 20 deposited structures were packed and minimized, following mutation, and used to generate 100 structures via implementation of the Backrub protocol for each input structure.³³ The final ensembles contained 2000 structure for each variant.

Calculating E_{FRET}. FRET efficiency (E_{FRET}) is dependent on the inverse 6th power of the donor-acceptor distance, as illustrated in the Förster Equation (Equation 1)¹

Quenching =
$$E_{FRET} = \frac{1}{1 + \left(\frac{R}{R_0}\right)^6}$$
 (1)

Here, R is the distance between the donor and acceptor chromophores, and R_0 is the Förster distance, the distance at which 50% of the energy is transferred. R_0 is specific to the pair of dye molecules and is given by

$$R_0^6 = \frac{(9000)\ln 10}{128\pi^5} \cdot \frac{\kappa^2 \Phi}{n^4 N_A} \cdot J_{PDA}$$
 (2)

where κ^2 is the orientation factor, Φ is the quantum yield of the donor in the absence of the acceptor, n is the refractive index of the solution, N_A is Avogadro's number, and J_{PDA} is the overlap integral of the normalized donor emission and acceptor absorption spectra.¹¹

The orientation factor κ^2 depends on the relative orientations of the donor emission transition dipole vector (\vec{D}) , the acceptor absorption transition dipole vector (\vec{A}) , and the vector connecting the centers of the two chromophores (\vec{R}) . ^{1,18} Defining θ_D as the angle between \vec{D} and \vec{R} , θ_A as the angle between \vec{A} and \vec{R} , and ϕ_{DA} as the dihedral angle formed by \vec{D} , \vec{A} and \vec{R} , κ^2 can then be

explicitly calculated using Equation 3, with a minimum theoretical value of 0 and a maximum of 4. As previously discussed, setting $\kappa^2 = 2/3$ yields the isotropic sampling approximation.

$$\kappa^2 = (\sin\theta_D \sin\theta_A \cos\phi_{DA} - 2\cos\theta_D \cos\theta_A)^2 \tag{3}$$

To improve the numerical accuracy of the computed Coulomb coupling, we make use of the TrESP method employed by Sobakinskaya and coworkers.¹² In this approach, *ab initio* transition densities, computed using Gaussian09, were fit to partial atomic charges for each heavy atom in each chromophore (represented as q_i and q_j in the donor (D) and acceptor (A), respectively) using Multiwfn.^{28, 36} The coupling was computed as the sum of all pairs of charge interactions between the donor and acceptor using Equation 4.¹²

$$J_{TrESP} = f \sum_{i,j} \frac{q_i^D q_j^A}{|R_i^D - R_j^A|}$$
 (4)

In the equation above, R_i and R_j represent the coordinates of charges q_i and q_j in the donor and acceptor, respectively. Lastly, the factor f accounts for local field effects and screening in an implicit manner and was set to unity for all calculations herein. Subsequently, J_{TrESP} is combined in Equation 5 with the calibration constant, C, to compute the rate constant of excitation energy coupling, k. The calibration constant takes into account the overlap integral of the chromophore pair via Equation 6.

$$k = |J_{TrESP}|^2 C (5)$$

$$C = \frac{3R_0^6}{2\tau_D} \frac{n^4}{(\mu_D)^2(\mu_A)^2} \tag{6}$$

In Equation 6, n is again the refractive index while μ_D and μ_A are the donor and acceptor dipoles computed from the transition charge and positions used in Equation 4. Lastly, the rate constant and donor lifetime, τ_D , then yield the E_{FRET} via Equation 7.^{1,12}

$$E_{FRET} = \frac{1}{1 + \frac{1}{\tau_D k}} \tag{7}$$

RESULTS AND DISCUSSION

Impact of PolyProline Sampling. Prior efforts focused on using MD simulations to develop a better understanding of the interaction between small fluorophores and thioamides. Although the distances extracted from these simulations were in reasonable agreement with the spectroscopic data, these simulations systematically underpredicted E_{FRET} and suggested that the average κ^2 in these polyproline peptides was ~ 1.1 , rather than the anticipated 2/3.24 We suspected that the MD simulations performed did not provide sufficient conformational sampling for effective E_{FRET} prediction and decided to perform simulations in PyRosetta, where a Monte Carlo approach would provide broad conformational sampling in a much more computationally efficient manner.

First, we used the dynamic isotropic approximation $\kappa^2 = 2/3$ (PDA, isotropic) and analyzed how varying sampling methods affects predicted E_{FRET} for the Cnf/Leu^s pair (Fig. 1a). With the PPII helix as a starting structure, limited torsion sampling on the backbone was performed via Backrubbased sampling, along with sidechain rotamer sampling.³²⁻³³ E_{FRET} values computed from structural

ensembles obtained using this sampling method showed poor correlations with experimental data (PPII in Fig. 1a-c), showing an RMSD of 0.16 under the PDA method in the isotropic limit. We suspected these issues stemmed from two problems, previously recognized in the literature. First, sidechain χ angle sampling in Rosetta, mainly through the PackRotamersMover, is optimized for positioning rotamers within well packed crystal structures.^{33, 37} Sampling approaches have been extended using the SidechainMover to generate conformer pools which are more representative of solution-phase sampling; however, we found here that the SidechainMover was prone to yield conformations trapped in local energy wells. Therefore, we increased the rate at which a random rotamer is selected during sampling and established that all χ angles were randomized at the start of the simulation (+ Chi Sampling in Fig. 1a–c). Next, we incorporated proline cis amide (cisPro) conformations, which have been observed in NMR experiments and the sampling of which has been shown to improve both FRET and photoinduced electron transfer predictions from simulations.²²⁻²³ We assessed the impact of introducing a uniform 2% probability of sampling cisPro conformations across all proline residues within the peptides (+ Internal cisPro in Fig. 1a– c) except for terminal prolines which were set at 10% cisPro probability based on NMR experiments (+ Terminal cisPro in Fig. 1a-c).^{22, 38} Overall, we observed that the successive addition of each of these sampling corrections did not afford any apparent improvement in the accuracy of our simulations, resulting in a reduction of only 0.05 in the E_{FRET} RMSD computed using the isotropic, PDA method.

Although corrections to cisPro conformational sampling have been widely reported to improve polyproline simulation accuracy, most of these experiments were performed using large dyes with flexible linkers. Therefore, we suspected that the proximity of the chromophores in our system to the backbone may introduce additional sampling concerns, as the chromophore orientations

become largely dependent on the allowed peptide backbone conformation. Indeed, separate studies by Zondlo and Basu demonstrated that placement of aromatic residues at the N- and C-termini of polyproline helices can result in significant increases in the population of cisPro conformations near the termini as a result of the formation of CH- π interactions between the proline beta-carbon and the aryl ring of the terminal residue (although these effects are admittedly modest for electron poor rings as in Cnf).³⁹⁻⁴¹ Therefore, this provides both an additional bias to the backbone conformations, in the form of increased cisPro propensities for prolines near the C-terminus, and perturbations in the χ angle sampling via conformational restriction of the chromophore to interactions with the backbone. To incorporate these changes, we designed a probabilistic sampling scheme based on previously reported cisPro propensities of terminal prolines and the fraction of structures which form CH- π interactions (+ CH- π Interaction in Fig. 1a–c).⁴⁰ By supplementing these values with observed χ angle population statistics from NMR experiments, we were able to probabilistically sample the correct torsion angles and propensities within our Monte-Carlo simulations. 38,40 Gratifyingly, we observed that the incorporation of CH- π interaction sampling significantly improves the correlation between our simulations and the observed FRET data (Fig 1b-d), reducing the RMSD for isotropic, PDA E_{FRET} calculations to 0.07. This result shows that incorporating subtle conformational effects from experimental observations can be important to accurate sampling of structural ensembles and hence accurate modeling of chromophore interactions.

Impact of Coulomb Coupling. While assaying the impact of different sampling schemes on the accuracy of our polyproline simulations, the impact of the E_{FRET} model was also explored. Three different methods were used to compute E_{FRET} from simulated structural ensembles. First, interprobe distances were used as inputs in the Förster equation under the isotropic limit of the

PDA (Eq. 1–2). Subsequently, dipole orientations were considered along with interprobe distances from each structure to compute an explicit version of PDA FRET (Eq. 1–3). Lastly, we used the TrESP method to account for the geometric complexities of Coulombic coupling at short range, computing pairwise interactions for every atom in each chromophore (Eq. 4–7).

We found a uniform impact of sampling on each E_{FRET} computation method (Fig. 1a–c). For all methods of computing E_{FRET} , incorporation of CH- π probabilistic sampling resulted in a significant boost in agreement between the predicted and experimental data. Curiously, under the most accurate sampling condition, we do not observe a large difference in the predictive accuracy between E_{FRET} values computed using the isotropic PDA approach and the most detailed TrESP method (Fig. 1d). The E_{FRET} RMSD values for the isotropic PDA and TrESP methods were 0.07 and 0.09, respectively, while the explicit PDA approach (Fig. 1b) is least correlative with the experimental data with an RMSD of 0.25. One explanation is that the isotropic PDA calculation averages out structural features that lead to inaccurate E_{FRET} measurements. The explicit PDA approach can have reasonable predictive power when the thioamide is positioned on a long, flexible sidechain, whose available conformational space is sampled by χ angle randomization. On the other hand, since the backbone thioamide can only explore limited rotational space, a more detailed computation is required to accurately capture the electronic interaction of the two chromophores, as we see for the TrESP model used here.

Impact of Conformational Restriction. In addition to the Cnf/Leu^s probe pair, where the thioamide is located within the peptide backbone, simulations were performed for a Cnf-Pro_n-Lys(Ac^s) polyproline series, where the thioamide was positioned at the end of the acetyl-lysine sidechain. We hypothesized that the conformational flexibility of the lysine sidechain would provide a useful comparison for understanding the potential impact of a relatively rigid orientation

for the backbone thioamide compared to traditional chromophores. Given that the donor and acceptor positions are swapped in the Cnf/Lys(Acs) experiments, compared to the previously described Cnf/Leu^s experiments, the CH- π interaction propensities and geometries were updated within the sampling scheme to reflect those observed in experiments containing N-terminal aromatic amino acids. 42-43 As in the Cnf/Leu^S simulation, the role of different methods for computing E_{FRET} and the impact of each sampling method was assessed for the Cnf/Lys(Ac^S) pair. Again, the isotropic PDA and TrESP compute methods perform similarly, producing RMSD of 0.07 compared to the experimental E_{FRET} values (Figure 2). Although the explicit PDA model provided a worse agreement with the experimental data (RMSD = 0.13), as was the case for the Cnf/Leu^s dataset, the difference in accuracy across all three compute methods was relatively minor (Figure 2d). Moreover, the differences resulting from sampling were also quite muted in the Cnf/Lys(Acs) dataset (Figure 2a–c). We suspect that this is likely due to the length of the Lys(Acs) sidechain, which when fully extended is ~ 9 Å from alpha-carbon to terminal methyl, compared to an alpha-carbon – alpha carbon distance of ~ 4 Å for prolines within the PPII helix. The long interprobe distance combined with the significant flexibility of side chains likely masks the contributions of cisPro and CH- π sampling.

To understand the molecular features that lead to the large discrepancy between the values computed using the isotropic and explicit PDA approaches for Cnf/Leu^S, additional analyses were performed on the κ^2 distributions from the most accurate structural ensembles (+ *CH-\piInteraction simulations*) of the Cnf/Leu^S and Cnf/AcLys^S series (Figure 3). Looking at the mean κ^2 values observed across all polyproline lengths (Fig. 3a), the average difference in κ^2 between the explicit PDA-based calculation and the implicit value (2/3) was ~ 0.2 for the Cnf/Leu^S series. The Cnf/Lys(Ac^S) series has an explicit κ^2 value of ~ 0.66 for all polyproline lengths and showed

minimal deviation between the explicit and implicit PDA E_{FRET} values. In contrast, the Cnf/Leu^s data have a noticeable difference in explicit and implicit PDA E_{FRET} values, attributable to the conformational restriction of the backbone thioamide dipole.

To further study the orientational difference between the backbone and sidechain thioamide datasets, a single polyproline length was selected for further analysis by decomposing κ^2 into its constitutive terms. The four-proline peptide was selected, as it showed the largest difference in κ^2 between the corresponding backbone and sidechain thioamide peptides (Fig. 3a). One can see clearly in Figure 3b that there is a significant difference between the isotropic and explicit κ^2 distributions for the Leu^S-Pro₄-Cnf peptide which is not as pronounced in the Cnf-Pro₄-Lys(Ac^S) peptide.¹⁸ The increase in κ^2 values less than 0.5 and depletion of κ^2 values greater than 1 results in the observed average κ^2 value of \sim 0.4 for the Cnf-Leu^S peptide.

Decomposition of the κ^2 distribution in terms of the component θ_D (Fig. 3c), φ_{DA} (Fig. 3d) and θ_A (Fig. 3e) distributions demonstrated that the conformational restriction of the backbone thioamide largely contributed to a change in the φ_{DA} distribution. For both the Leu^S-Pro₄-Cnf and Cnf-Pro₄-Lys(Ac^S) peptides we observed that the θ_D (Fig. 3c) distribution can be fit to a gaussian distribution, which is expected for the isotropic limit. We suspect that the small differences between the backbone and sidechain distributions likely arise from differences in the CH- π interactions experienced at the N and C-termini.¹⁸ Furthermore, we observed that the θ_A distributions (Fig. 3e) are quite similar between the Cnf/Leu^S and Cnf/AcLys^S series. Initially, we found it curious that even for the sidechain thioamide peptide, the θ_A distribution is not broad and gaussian in nature like the θ_D distribution. Analysis of the Cnf-Pro₄-Lys(Ac^S) structures showed that a variety of sidechain Lys(Ac^S) conformations were indeed sampled, but that since θ_D and θ_A are primarily dependent on the structure of the chromophore, their distributions are not

significantly affected by increased conformational flexibility (see SI, Fig. S1 and associated discussion). 18 Moreover, we observed a clear difference in the φ_{DA} distributions (Fig 3d). The sidechain thioamide upholds the expected uniform distribution for isotropic sampling, while the backbone thioamide polyproline peptide has several preferred dihedral angles.¹⁸ Thus, obtaining a κ^2 value near the isotropic ideal for Cnf-Pro₄-Lys(Ac^S) is primarily the result of changes in the ϕ_{DA} distribution.⁴⁴ If we track the most populated θ_A bin following histogram analysis of each polyproline peptide (Fig. 3f) we observe a damped three residue periodicity, matching the threefold symmetry of the PPII helix. This periodicity is observed for both the backbone and sidechain thioamide, further supporting the previous conclusion that the θ_A distribution is primarily dependent on the chromophore structure. However, this effect does not necessarily influence κ^2 . Although the θ_A bin values follow a similar pattern for both the Cnf/Leu^S and Cnf/AcLys^S series, the Cnf/AcLys^S series κ^2 values are essentially invariant. Taken together, these data show that proper representation of conformational restriction plays a major role in the ability to predict FRET for backbone thioamides, but a minor role for sidechain thioamides. However, explicit modeling of restricted conformations must be accompanied by the inclusion of coulombic coupling to accurately capture the influence of the sampled states.

Effects of conformational sampling and Coulomb coupling on Tyr FRET modeling. To extend our findings from the Cnf-thioamide probe pair systems, we performed the same simulations with the Tyr/Leu^S pair (Fig. 4). We again observe that the sampling method accounting for CH- π interactions between the terminal aromatic chromophore and the proline backbone greatly enhances correlation with experimental E_{FRET} values (Fig. 4a–c). Additionally, we again observe that the isotropic PDA approach and the TrESP approach correlate comparably with experimental data (Fig. 4d), showing that this system is similarly impacted by thioamide rotational

restriction and that more complex treatment of Coulombic interactions is necessary once explicit calculation of κ^2 is included.

Absence of FRET in Trp/thioamide pairs. Unlike the Cnf/thioamide and Tyr/thioamide FRET pairs, Trp/thioamide fluorescence data are not well-correlated with predictions from the overlap of donor fluorescence emission and acceptor absorbance spectra.²⁴⁻²⁵ Therefore, we wanted to confirm that the discrepancy did not arise from a failure to account for Coulomb coupling in previous simulations of the Trp/Leu^S and Trp/Lys(Ac^S) series. We see that use of the TrESP model does result in higher computed FRET efficiencies than the PDA-based calculations, but that these values still dramatically underpredict the experimental quenching values (Fig. 5a-b). We again observed that placement of the thioamide on the lysine sidechain diminishes the differences between combinations of sampling and FRET calculation methods, and corroborates the finding from the Trp/Leu^s peptides that FRET-based computes do not effectively describe the observed experimental fluorescence quenching (Fig. S2). Therefore, these calculations support our earlier assertions that Trp quenching by thioamides occurs through a Dexter mechanism.²⁵ Indeed, modeling quenching based on Dexter energy transfer provides reasonable fits across all sampling methods (Fig 5c-d). While this does not rule out the possibility of an electron transfer process, the formal similarity of simple electron transfer equations and the Dexter model prevents us from distinguishing between these two models with our existing data (see SI for additional discussion) and therefore we have used the Dexter fit for subsequent analysis.

FRET Predictions in a Protein System. Experimentally determined E_{FRET} values from thioamide-induced quenching in full-sized proteins have been similarly difficult to predict from earlier MD-based structural modeling.⁴ Based on our findings above, we hypothesized that introduction of the improved calculation of Coulombic coupling using the TrESP model would

provide better correlations between the experimental and computational E_{FRET} values. Previous experimental studies have utilized fluorescently labeled CaM binding to a thioamide containing pOCNC peptide as a model system for studying thioamide induced fluorescence quenching in the context of a protein (Fig. 6a).^{4,25} Previous attempts to model Cnf and Tyr FRET based on the 20 lowest energy structures of the CaM/pOCNC complex derived from NMR experiments found moderate levels of agreement for Cnf experiments, but much poorer agreement for Tyr experiments.^{4, 25} To determine whether insufficient conformational sampling was responsible for these inconsistencies, the complexes were simulated using a PyRosetta-based method which utilized Backrub motions to generate a conformational ensemble representative of solution phase sampling.³² Unlike the polyproline simulations, we were not able to explicitly assess the impact of sampling on prediction accuracy, as the requisite experimental data was not identified for the CaM/pOCNC complex. From these ensembles, we computed E_{FRET} values using the isotropic and explicit PDA approaches as well as the TrESP method (Fig. 6b). The quantum yield corresponding to each Cnf, Tyr and Trp labeling position were taken from the initial published values, except in the case of Cnf13 where the free chromophore value (0.11) produced significantly improved correlations over the previously published value (0.003) between simulated and experimental EFRET values.^{25,45} Overall, predictions from the TrESP approach for Cnf and Tyr provided more accurate values, with an RMSD of 0.14 compared to 0.21 and 0.25 for the isotropic and explicit PDA methods, respectively. However, for 2 of the 9 Cnf and Tyr pairs, the TrESP method performed slightly worse than the PDA-based calculations. Lastly, we examined Trp quenching using the Dexter model equation, with parameters fit to the + CH- π Interaction polyproline simulations. We observed that fluorescence quenching of CaM Trp mutants is well predicted by this parameterized Dexter model and that again little to no FRET is predicted.

While the exact reason underlying the observation that the TrESP method does not universally outperform the PDA-based calculation is unclear, several potential explanations can be provided. The E_{FRET} values calculated using PDA, explicit or or TrESP method are reliant on the accurate sampling of sidechain orientations, as \varkappa^2 is defined by the relative orientation of transition dipoles. Therefore, incomplete sampling of local conformations around the labelling site in the lowest-energy NMR structures of CaM/pOCNC can impair the accuracy of TrESP method, while PDA, isotropic method is free of such limitations. This dependence may be generalized to other protein systems, although that is not explicitly validated here. It is also possible that complexities in the photophysical properties of the thioamide are limiting the accuracy of the explicit calculation of \varkappa^2 . For example, the thioamide absorbance profile can be sensitive to its local environment, including solvent accessibility and electronic interactions with neighboring residues that could be influenced by events like pOCNC binding to CaM. 46-47 Nonetheless, overall we observe that implementing the TrESP method improves FRET prediction in our model protein system.

Overall, the results from the CaM/pOCNC system further support the hypothesis that complete conformational sampling and accounting for Coulomb coupling allows one to more accurately predict Cnf or Tyr FRET to thioamides.

CONCLUSIONS

To date, most experimental and computational studies focusing on FRET have utilized visible wavelength fluorophores with long working ranges (R_0 of 30-50 Å) attached to proteins via relatively flexible linkers. For such chromophores, the isotropic PDA model is often sufficient. Thioamide FRET pairs, on the other hand, have short R_0 values of 12-15 Å and backbone probes are certainly conformationally restricted so that the PDA model is not valid and additional factors

much be considered. In our efforts to accurately predict E_{FRET} for Cnf quenching by backbone (Cnf/Leu^S) and sidechain thioamides (Cnf/Lys(Ac^S)), we found that the conformational restriction of the backbone thioamide significantly affects the E_{FRET} values simulated via PyRosetta. Conformational restriction results in non-isotropic sampling of the dihedral angle between the donor and acceptor transition dipoles. The restricted motion also conveys an enhanced sensitivity of the backbone thioamide to the populations of cisPro motifs resulting from CH- π interactions between aromatic sidechains and proline residues.^{22,40}

Additionally, we have observed that for both the Cnf/Leu^s and Tyr/Leu^s polyproline series the TrESP approach, which provides a more realistic description of transition dipole interactions at short interchromophore distances, provides accurate ensemble E_{FRET} predictions from single-structure computes. Similarly, representing Coulomb coupling with the TrESP approach significantly improved the correlation between predicted and experimentally observed FRET efficiencies for Cnf- and Tyr/thioamide interactions observed in CaM.

We have also utilized the improved accuracy of the Cnf and Tyr simulations to study the mechanism by which thioamides quench Trp fluorescence and how generalizable the role of Coulomb coupling is to more complex protein systems. None of the tested methods for computing a FRET-based interaction was able to reproduce experimentally observed Trp quenching in polyproline or CaM systems. However, a simple Dexter transfer model provided a good fit to the polyproline data, and once parameterized, could accurately predict the fluorescence quenching observed in the CaM-pOCNC simulations.

Overall, this work demonstrates that improved modeling of FRET interactions can be achieved by accounting for (1) unique conformational constraints in a given system and (2) short-range FRET interactions by incorporation of TrESP modelling. While these considerations become less

important when the dynamic isotropic approximation is valid, they are important for small, inflexible thioamide-based dyes and are likely to be comparably important for other minimalist fluorophores with relatively short working ranges such as Trp or methoxycoumarinyl alanine paired with acridonylalanine.⁴⁸⁻⁵⁰ The implementation described here is not very computationally demanding and could be applied to these FRET pairs as well.

FIGURES

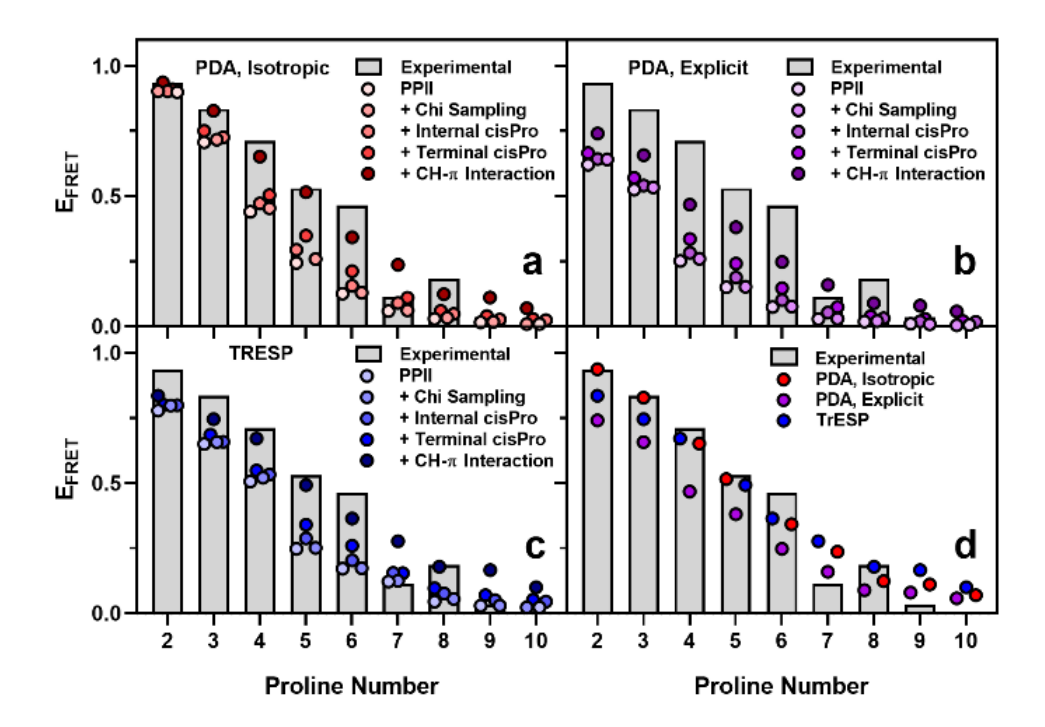


Figure 1. Predicted E_{FRET} values from simulations of the Leu^S-Pro_n-Cnf system compared to experimental values.²⁴ Efficacy of each sampling approach (+ Chi Sampling, + Internal cisPro, + Terminal cisPro, + CH-π Interaction) was assessed for all three methods of computing E_{FRET} , (a) PDA, isotopic; (b) PDA, explicit; and (c) TrESP, to determine the most accurate sampling method. (d) The accuracy of all three approaches for computing E_{FRET} is compared using the + CH-π Interaction conformational ensemble.

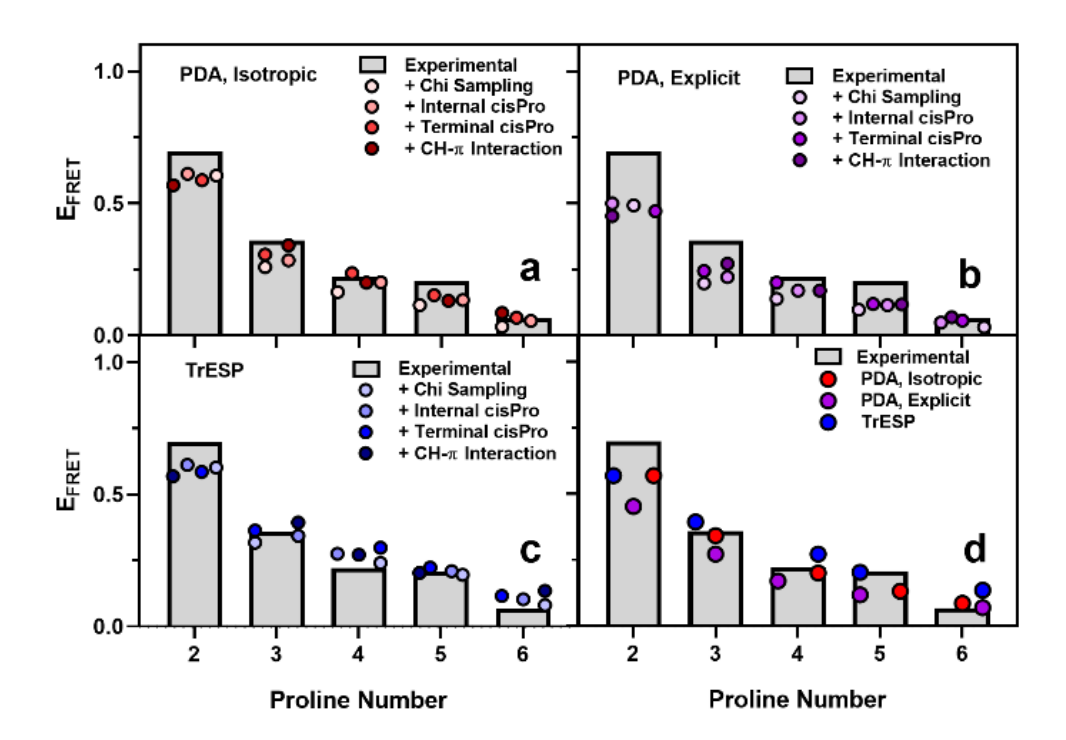


Figure 2. Predicted E_{FRET} values from simulations of the Cnf-Pro_n-Lys(Ac^S) system compared to experimental values.³¹ Efficacy of each sampling approach (+ Chi Sampling, + Internal cisPro, + Terminal cisPro, + CH- π Interaction) was assessed for all three methods of computing E_{FRET} , (a) PDA, isotopic; (b) PDA, explicit; and (c) TrESP, to determine the most accurate sampling method. (d) The accuracy of all three approaches for computing E_{FRET} is compared using the + CH- π Interaction conformational ensemble.

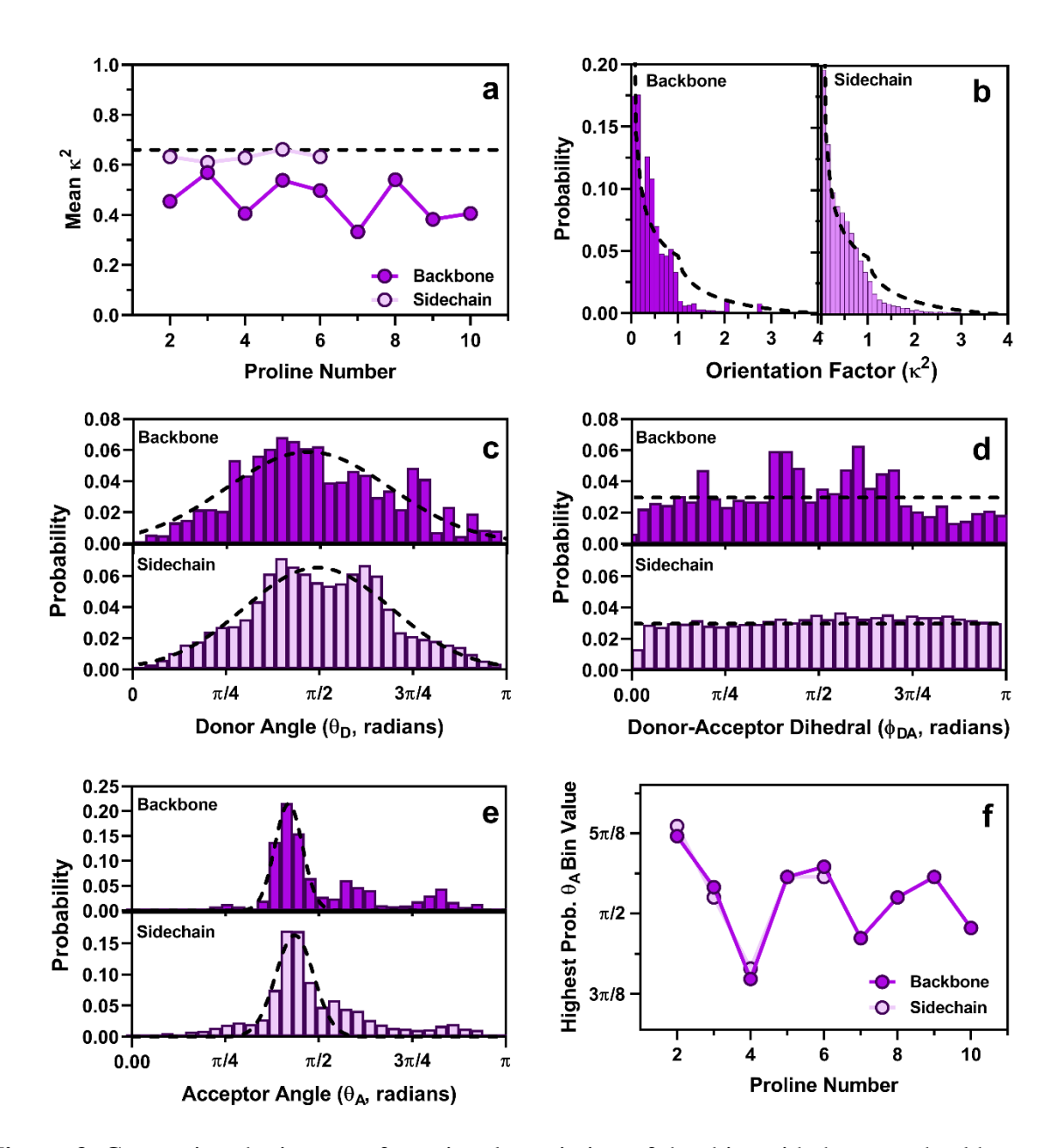


Figure 3. Comparing the impact of rotational restriction of the thioamide between backbone and sidechain incorporation. Various parameters were computed from each value (θ_D , θ_A , ϕ_{DA}) used to compute κ^2 from the Leu^S-Pro₄-Cnf (Backbone) and Cnf-Pro₄-Lys(Ac^S) (Sidechain) + CH-π Interaction simulations. (a) The mean κ^2 value was computed across all Cnf/thioamide polyproline peptides. Histograms of the (b) κ^2 , (c) θ_D , (d) ϕ_{DA} and (e) θ_A were computed for Leu^S-Pro₄-Cnf and Cnf-Pro₄-Lys(Ac^S) to observe the impact of the donor and acceptor sampling on the resultant κ^2 distribution. Dashed lines mark (a) $\kappa^2 = 2/3$ and represent expected isotropic distributions of (b) κ^2 and (d) ϕ_{DA} , while dashed lines in (c) θ_D and (e) θ_A plots are Gaussian fits to the respective data. (f) Extraction of the most populated θ_A value for each Cnf/thioamide peptide revealed a damped periodic function derived from the 3-fold symmetry of the PPII helix. All angles are reported in radians.

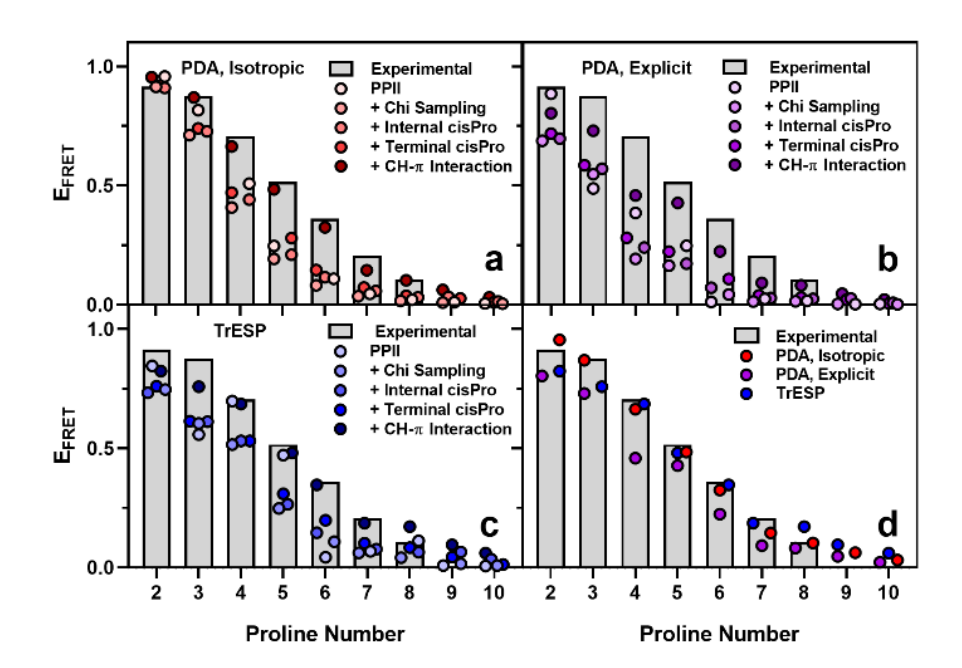


Figure 4. Predicted E_{FRET} values from simulations of the Leu^S-Pro_n-Tyr system compared to experimental values.²⁵ Efficacy of each sampling approach (+ Chi Sampling, + Internal cisPro, + Terminal cisPro, + CH-π Interaction) was assessed for all three methods of computing E_{FRET} , (a) PDA, isotopic; (b) PDA, explicit; and (c) TrESP, to determine the most accurate sampling method. (d) The accuracy of all three approaches for computing E_{FRET} is compared using the + CH-π Interaction conformational ensemble.

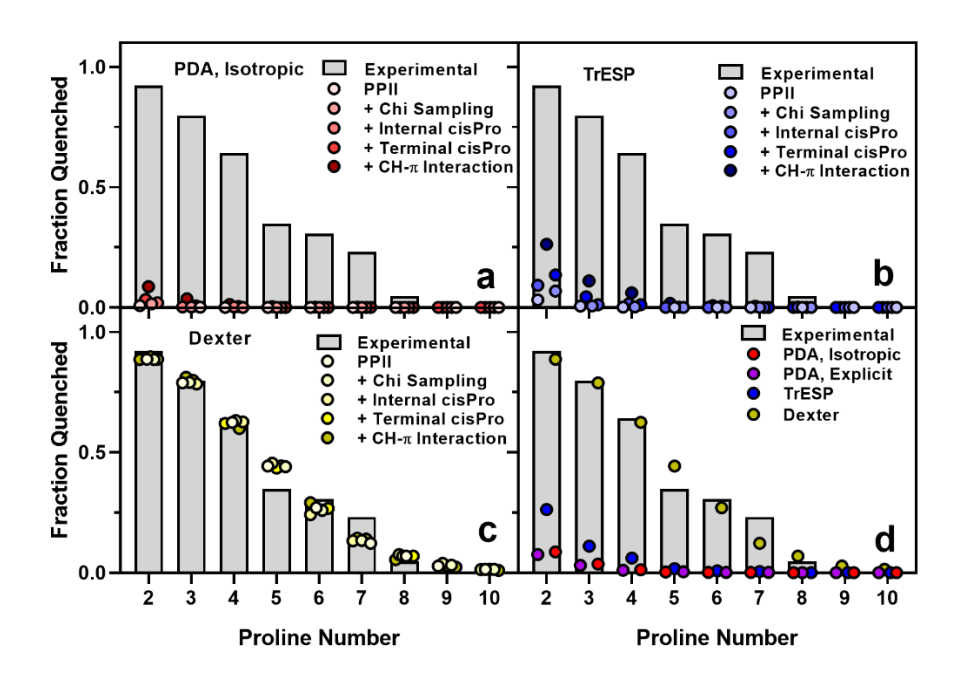
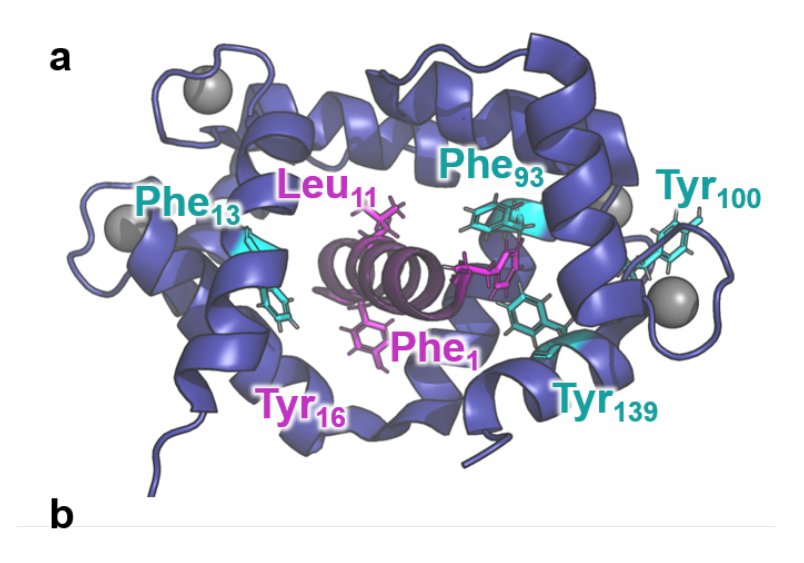


Figure 5. Predicted quenching efficiency values from simulations of the Leu^S-Pro_n-Trp system compared to experimental values.²⁵ The impact of sampling on the predicted quenching (E_{FRET}) values for the (a) PDA, isotopic and (b) TrESP E_{FRET} calculation methods was compared along corresponding quenching predictions using (c) a fitted Dexter model. (d) The accuracy of the three approaches for computing E_{FRET} (PDA, isotopic; PDA, explicit; TrESP) as well as a Dexter quenching model is compared for the + CH-π Interaction conformational ensemble.²⁵



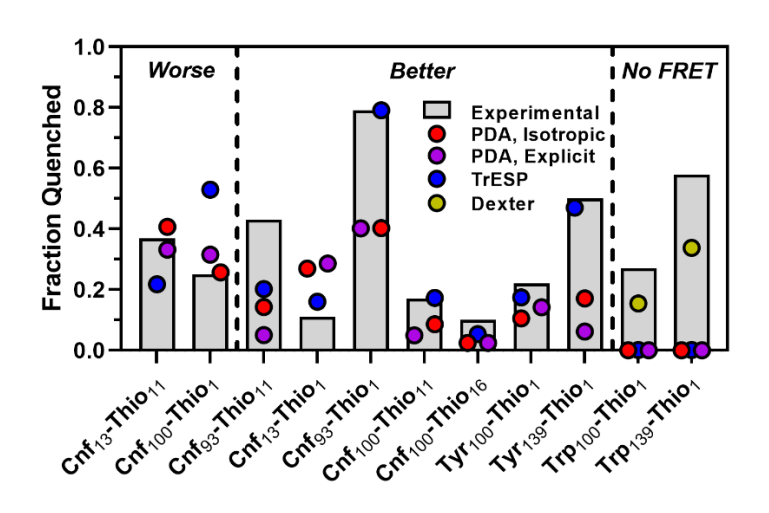


Figure 6. Distance dependent quenching of CaM fluorescence by a bound thioamide containing pOCNC peptide. (a) Representation showing the pOCNC peptide (purple) bound to CaM (dark blue) along with the donor fluorophore (cyan) and thioamide (pink) labeling positions. (b) Comparison to experimental quenching for all three approaches for computing E_{FRET} (PDA, Isotropic; PDA, Explicit; and TrESP) for Cnf and Tyr CaM mutants, along with Dexter predictions for CaM Trp mutants. (24-25)

ASSOCIATED CONTENT

Supporting Information. The following files are available free of charge. Simulation details, sampling methods, additional data from experimental comparisons, methods for computing E_{FRET} , details from Gaussian simulations, and details from Multiwfn analysis for computing atomic transition charges. (PDF)

AUTHOR INFORMATION

Corresponding Author

* JJF: jferrie@berkeley.edu; EJP: ejpetersson@sas.upenn.edu

Present Addresses

† Department of Chemistry, Massachusetts Institute of Technology, Cambridge, Massachusetts, 02139, United States

‡ Department of Molecular & Cell Biology, University of California, Berkeley, Berkeley, California, 94720, United States

Author Contributions

JJF and JY performed all computational simulations and comparisons to experimental data. All authors contributed to writing the manuscript.

Notes

All simulation and analysis scripts as well as demonstration simulations are available on Github: https://github.com/jferrie3/Thioamide-PolyProline-PyRosetta.

ACKNOWLEDGMENT

This work was supported by funding from the University of Pennsylvania and the National Science Foundation (NSF CHE-1708759 to E.J.P.). JJF thanks the National Science Foundation (NSF DGE-1321851) and the Parkinson's Disease Foundation (PF-RVSA-SFW-1754) for fellowship support. JY thanks the University of Pennsylvania Center for Undergraduate and Research Fellowships and Roy and Diana Vagelos Science Challenge Award for fellowship support. We are grateful to David Baker and his laboratory for guidance of JJF during his summer internship.

ABBREVIATIONS

CaM, calmodulin; Cnf, p-cyanophenylalanine; cisPro, cis amide containing proline; E_{FRET} , FRET efficiency; FRET, Förster resonance energy transfer; MD, molecular dynamics; pOCNC, peptide taken from an olfactory, cyclic, nucleotide gated ion channel; PPII, polyproline type-II; Lys(Acs), thioacetyl lysine; Leus, thioleucine; TrESP, Transition Electro-static Potential; Trp, tryptophan; Tyr, tyrosine;

REFERENCES

- 1. Lakowicz, J. R., *Principles of Fluorescence Spectroscopy*. 3rd ed.; Springer: New York, NY, USA, 2006.
- 2. Yguerabide, J.; Foster, M. C., Fluorescence Spectroscopy of Biological Membranes. *Mol. Biochem. Biophys.* **1981,** *31*, 199-269.
- 3. Tyagi, S.; Lemke, E. A., Single-Molecule Fret and Crosslinking Studies in Structural Biology Enabled by Noncanonical Amino Acids. *Curr. Opin. Struct. Biol.* **2015**, *32*, 66-73.
- 4. Wissner, R. F.; Batjargal, S.; Fadzen, C. M.; Petersson, E. J., Labeling Proteins with Fluorophore/Thioamide Förster Resonant Energy Transfer Pairs by Combining Unnatural Amino Acid Mutagenesis and Native Chemical Ligation. *J. Am. Chem. Soc.* **2013**, *135*, 6529-6540.
- 5. Winkler, R. G.; Keller, S.; Radler, J. O., Intramolecular Dynamics of Linear Macromolecules by Fluorescence Correlation Spectroscopy. *Phys. Rev. E* **2006**, *73*, 041919.
- 6. Syed, S.; Pandey, M.; Patel, S. S.; Ha, T., Single-Molecule Fluorescence Reveals the Unwinding Stepping Mechanism of Replicative Helicase. *Cell Rep.* **2014**, *6*, 1037-1045.
- 7. Favicchio, R.; Dragan, A. I.; Kneale, G. G.; Read, C. M., Fluorescence Spectroscopy and Anisotropy in the Analysis of DNA-Protein Interactions. *Methods Mol. Biol.* **2009**, *543*, 589-611.
- 8. Martin, S. F.; Tatham, M. H.; Hay, R. T.; Samuel, I. D., Quantitative Analysis of Multi-Protein Interactions Using Fret: Application to the Sumo Pathway. *Protein Sci.* **2008**, *17*, 777-784.
- 9. Yang, L.; Schepartz, A., Relationship between Folding and Function in a Sequence-Specific Miniature DNA-Binding Protein. *Biochemistry* **2005**, *44*, 7469-7478.
- 10. Dobson, C. M., Protein Folding and Misfolding. *Nature* **2003**, *426*, 884-890.
- 11. Clegg, R. M., Reviews in Fluorescence. Springer: New York, 2006; Vol. 3.
- 12. Sobakinskaya, E.; Schmidt am Busch, M.; Renger, T., Theory of Fret "Spectroscopic Ruler" for Short Distances: Application to Polyproline. *J. Phys. Chem. B* **2018**, *122*, 54-67.
- 13. Ferrie, J. J.; Haney, C. M.; Yoon, J.; Pan, B.; Lin, Y.-C.; Fakhraai, Z.; Rhoades, E.; Nath, A.; Petersson, E. J., Using a Fret Library with Multiple Probe Pairs To drive Monte Carlo Simulations of A-Synuclein. *Biophys. J.* **2018**, *114*, 53-64.
- 14. van der Meer, B. W., Kappa-Squared: From Nuisance to New Sense. *J. Biotechnol.* **2002**, 82, 181-196.
- 15. Dale, R. E.; Eisinger, J.; Blumberg, W. E., The Orientational Freedom of Molecular Probes. The Orientation Factor in Intramolecular Energy Transfer. *Biophys. J.* **1979**, *26*, 161-193.
- 16. Ivanov, V.; Li, M.; Mizuuchi, K., Impact of Emission Anisotropy on Fluorescence Spectroscopy and Fret Distance Measurements. *Biophys. J.* **2009**, *97*, 922-929.
- 17. Khrenova, M.; Topol, I.; Collins, J.; Nemukhin, A., Estimating Orientation Factors in the Fret Theory of Fluorescent Proteins: The Tagrfp-Kfp Pair and Beyond. *Biophys. J.* **2015**, *108*, 126-132.
- 18. Loura, L. M. S., Simple Estimation of Forster Resonance Energy Transfer (Fret) Orientation Factor Distribution in Membranes. *Int J Mol Sci* **2012**, *13*, 15252-15270.
- 19. Wu, P.; Brand, L., Orientation Factor in Steady-State and Time-Resolved Resonance Energy Transfer Measurements. *Biochemistry* **1992**, *31*, 7939-7947.
- 20. Peulen, T. O.; Opanasyuk, O.; Seidel, C. A. M., Combining Graphical and Analytical Methods with Molecular Simulations to Analyze Time-Resolved Fret Measurements of Labeled Macromolecules Accurately. *J. Phys. Chem. B* **2017**, *121*, 8211-8241.

- 21. Doose, S.; Neuweiler, H.; Barsch, H.; Sauer, M., Probing Polyproline Structure and Dynamics by Photoinduced Electron Transfer Provides Evidence for Deviations from a Regular Polyproline Type Ii Helix. *Proc. Natl. Acad. Sci. USA* **2007**, *104*, 17400-17405.
- 22. Best, R. B.; Merchant, K. A.; Gopich, I. V.; Schuler, B.; Bax, A.; Eaton, W. A., Effect of Flexibility and Cis Residues in Single-Molecule Fret Studies of Polyproline. *Proc. Natl. Acad. Sci. USA* **2007**, *104*, 18964-18969.
- 23. Haenni, D.; Zosel, F.; Reymond, L.; Nettels, D.; Schuler, B., Intramolecular Distances and Dynamics from the Combined Photon Statistics of Single-Molecule Fret and Photoinduced Electron Transfer. *J. Phys. Chem. B* **2013**, *117*, 13015-13028.
- 24. Goldberg, J. M.; Batjargal, S.; Petersson, E. J., Thioamides as Fluorescence Quenching Probes: Minimalist Chromophores to Monitor Protein Dynamics. *J. Am. Chem. Soc.* **2010**, *132*, 14718-14720.
- 25. Goldberg, J. M.; Wissner, R. F.; Klein, A. M.; Petersson, E. J., Thioamide Quenching of Intrinsic Protein Fluorescence. *Chem. Commun.* **2012**, *48*, 1550-1552.
- 26. Goldberg, J. M.; Batjargal, S.; Chen, B. S.; Petersson, E. J., Thioamide Quenching of Fluorescent Probes through Pho-Toinduced Electron Transfer: Mechanistic Studies and Applications. *J. Am. Chem. Soc.* **2013**, *135*, 18651–18658.
- 27. Chaudhury, S.; Lyskov, S.; Gray, J. J., Pyrosetta: A Script-Based Interface for Implementing Molecular Modeling Algorithms Using Rosetta. *Bioinformatics* **2010**, *26*, 689-691.
- 28. Frisch, M. J.; Trucks, G. W.; Schlegel, H. B.; Scuseria, G. E.; Robb, M. A.; Cheeseman, J. R.; Scalmani, G.; Barone, V.; Mennucci, B.; Petersson, G. A., et al. *Gaussian 09*, Gaussian, Inc.: Wallingford, CT, USA, 2009.
- 29. Renfrew, P. D.; Choi, E. J.; Bonneau, R.; Kuhlman, B., Incorporation of Noncanonical Amino Acids into Rosetta and Use in Computational Protein-Peptide Interface Design. *PLoS One* **2012**, *7*, e32637.
- 30. Breneman, C. M.; Wiberg, K. B., Determining Atom-Centered Monopoles from Molecular Electrostatic Potentials. The Need for High Sampling Density in Formamide Conformational Analysis. *J. Comput. Chem.* **1990,** *11*, 361-373.
- 31. Robkis, D. M.; Hoang, E. M.; Po, P.; Deutsch, C. J.; Petersson, E. J., Side-Chain Thioamides as Fluorescence Quenching Probes. *Biopolymers* **2020**.
- 32. Smith, C. A.; Kortemme, T., Backrub-Like Backbone Simulation Recapitulates Natural Protein Conformational Variability and Improves Mutant Side-Chain Prediction. *J. Mol. Biol.* **2008**, *380*, 742-756.
- 33. Smith, C. A.; Kortemme, T., Predicting the Tolerated Sequences for Proteins and Protein Interfaces Using Rosettabackrub Flexible Backbone Design. *PLOS ONE* **2011**, *6*, e20451.
- 34. Alford, R. F.; Leaver-Fay, A.; Jeliazkov, J. R.; O'Meara, M. J.; DiMaio, F. P.; Park, H.; Shapovalov, M. V.; Renfrew, P. D.; Mulligan, V. K.; Kappel, K., et al., The Rosetta All-Atom Energy Function for Macromolecular Modeling and Design. *J. Chem. Theory Comput.* **2017**, *13*, 3031-3048.
- 35. Contessa, G. M.; Orsale, M.; Melino, S.; Torre, V.; Paci, M.; Desideri, A.; Cicero, D. O., Structure of Calmodulin Complexed with an Olfactory Cng Channelfragment and Role of the Central Linker: Residual Dipolar Couplingsto Evaluate Calmodulin Binding Modes Outside the Kinase Family. *J. Biomol. NMR* **2005**, *31*, 185-199.
- 36. Lu, T.; Chen, F., Multiwfn: A Multifunctional Wavefunction Analyzer. *J. Comput. Chem.* **2012,** *33*, 580-592.

- 37. Kellogg, E. H.; Leaver-Fay, A.; Baker, D., Role of Conformational Sampling in Computing Mutation-Induced Changes in Protein Structure and Stability. *Proteins* **2011**, *79*, 830-838.
- 38. Nardi, F.; Kemmink, J.; Sattler, M.; Wade, R. C., The Cisproline(I 1)-Aromatic(I) Interaction: Folding of the Ala-Cispro-Tyr Peptide Characterized by Nmr and Theoretical Approaches. *J. Biomol. NMR* **2000**, *17*, 63-77.
- 39. Dasgupta, B.; Chakrabarti, P.; Basu, G., Enhanced Stability of Cis Pro-Pro Peptide Bond in Pro-Pro-Phe Sequence Motif. *FEBS Lett.* **2007**, *581*, 4529-4532.
- 40. Ganguly, H. K.; Majumder, B.; Chattopadhyay, S.; Chakrabarti, P.; Basu, G., Direct Evidence for Ch···Π Interaction Mediated Stabilization of Pro-Cispro Bond in Peptides with Pro-Pro-Aromatic Motifs. *J. Am. Chem. Soc.* **2012**, *134*, 4661-4669.
- 41. Zondlo, N. J., Aromatic–Proline Interactions: Electronically Tunable Ch/ Π Interactions. *Acc. Chem. Res.* **2013**, *46*, 1039-1049.
- 42. Wu, W. J.; Raleigh, D. P., Local Control of Peptide Conformation: Stabilization of Cis Proline Peptide Bonds by Aromatic Proline Interactions. *Biopolymers* **1998**, *45*, 381-394.
- 43. Reimer, U.; Scherer, G.; Drewello, M.; Kruber, S.; Schutkowski, M.; Fischer, G., Side-Chain Effects on Peptidyl-Prolyl Cis/Trans Isomerisation. *J. Mol. Biol.* **1998**, 279, 449-460.
- 44. van der Meer, B. W.; van der Meer, D. M.; Vogel, S. S., Optimizing the Orientation Factor Kappa-Squared for More Accurate Fret Measurements. *FRET Förster Resonance Energy Transfer* **2013**, 63-104.
- 45. Wissner, R. F.; Batjargal, S.; Fadzen, C. M.; Petersson, E. J., Labeling Proteins with Fluorophore/Thioamide Forster Resonant Energy Transfer Pairs by Combining Unnatural Amino Acid Mutagenesis and Native Chemical Ligation. *J Am Chem Soc* **2013**, *135*, 6529-6540.
- 46. Walters, C. R.; Ferrie, J. J.; Petersson, E. J., Dithioamide Substitutions in Proteins: Effects on Thermostability, Peptide Binding, and Fluorescence Quenching in Calmodulin. *Chem. Commun.* **2018**, *54*, 1766-1769.
- 47. Huang, Y.; Ferrie, J. J.; Chen, X.; Zhang, Y.; Szantai-Kis, D. M.; Chenoweth, D. M.; Petersson, E. J., Electronic Interactions of I, I + 1 Dithioamides: Increased Fluorescence Quenching and Evidence for N-to-Π* Interactions. *Chem. Commun.* **2016**, *52*, 7798-7801.
- 48. Ferrie, J. J.; Ieda, N.; Haney, C. M.; Walters, C. R.; Sungwienwong, I.; Yoon, J.; Petersson, E. J., Multicolor Protein Fret with Tryptophan, Selective Coumarin-Cysteine Labeling, and Genetic Acridonylalanine Encoding. *Chem. Commun.* **2017**, *53*, 11072-11075.
- 49. Speight, L. C.; Muthusamy, A. K.; Goldberg, J. M.; Warner, J. B.; Wissner, R. F.; Willi, T. S.; Woodman, B. F.; Mehl, R. A.; Petersson, E. J., Efficient Synthesis and in Vivo Incorporation of Acridon-2-Ylalanine, a Fluorescent Amino Acid for Lifetime and Förster Resonance Energy Transfer/Luminescence Resonance Energy Transfer Studies. *J. Am. Chem. Soc.* **2013**, *135*, 18806-18814.
- 50. Sungwienwong, I.; Ferrie, J. J.; Jun, J. V.; Liu, C.; Barrett, T. M.; Hostetler, Z. M.; Ieda, N.; Hendricks, A.; Muthusamy, A. K.; Kohli, R. M., et al., Improving the Fluorescent Probe Acridonylalanine through a Combination of Theory and Experiment. *J. Phys. Org. Chem.* **2018**, *31*, e3813.

TOC GRAPHIC

